



Biomechanical comparison of knotless wide suture double-row SutureBridge rotator cuff repair to double-row standard suture repair

Victor K. Liu, BSc(Med)^a, Theresia M. Bouwmeester, MSc^b,
Geoffrey C.S. Smith, MBChB, FRACS, FAOrthoA^{a,c}, Patrick H. Lam, MD, PhD^{a,c,d,*}

^aUniversity of New South Wales, Sydney, NSW, Australia

^bFaculty of Medicine, Leiden University, Leiden, The Netherlands

^cSt George Orthopaedic Department, Sydney, NSW, Australia

^dOrthopaedic Research Institute, Sydney, NSW, Australia

Background: A comparison of self-reinforcement and footprint compression between standard- and wide-diameter suture material in double-row SutureBridge repair techniques has not been performed. The aim of this study was to compare the self-reinforcement and footprint contact pressure generated under progressive tensile loads between 2 double-row SutureBridge rotator cuff repair techniques: 1 performed with FiberWire and 1 performed with FiberTape in a knotless technique.

Materials and methods: Rotator cuff repairs were performed in 10 pairs of ovine shoulders. One group underwent a double-row SutureBridge repair using FiberWire. The other group underwent an identical repair with FiberTape. Footprint contact pressure was measured from 0° to 60° of abduction under loads of 0-60 N. Pull-to-failure tests were then performed.

Results: In both repair constructs at 0° of abduction, each 10-N increase in rotator cuff tensile load led to a significant increase in footprint contact pressure ($P < .05$). The rate of increase in footprint contact pressure was greater in the FiberTape construct (ratio, 1.68; $P = .00035$). In both repair constructs, the highest values for footprint contact pressure were seen at 0° of abduction. No difference in pull to failure, peak load, or total energy was found between the groups.

Conclusion: Self-reinforcement was seen in both double-row SutureBridge repairs with standard- and wide-diameter suture material but was greater in the repair with the wide-diameter suture material construct. Footprint compression is greater in a knotless double-row SutureBridge repair with wide-diameter suture material than in a knotted double-row SutureBridge repair with standard-diameter suture material at 20° of abduction.

Level of evidence: Basic Science Study; Biomechanics

© 2020 Journal of Shoulder and Elbow Surgery Board of Trustees. All rights reserved.

Keywords: Rotator cuff tear; arthroscopic rotator cuff repair; self-reinforcement; double row; SutureBridge; suture diameter

Rotator cuff tears are a common cause of shoulder pain, loss of power, and diminished upper-limb function.^{3,7}

Institutional review board was not required for this basic science study.

*Reprint requests: Patrick H. Lam, MD, PhD, Biomechanics, Orthopaedic Research Institute, St George Hospital Campus, Level 2, 4-10 South Street, Kogarah, NSW 2217, Australia.

E-mail address: patlam.ori@gmail.com (P.H. Lam).

Advances in repair methods have improved the clinical outcomes of rotator cuff repair surgery and have reduced the incidence of rotator cuff retears.⁴ In rotator cuff repair, self-reinforcement is a mechanism whereby increasing tension applied to the repair construct generates increasing resistance to structural failure by generating a progressive increase in the compressive forces at the tendon

footprint.^{1,5,6} The compressive forces created at the footprint increase the frictional resistance between the tendon and bone, thereby reducing gap formation between the 2 surfaces. Baseline footprint compression in double-row SutureBridge (Arthrex, Naples, FL, USA) rotator cuff repair is generated by the bridging sutures. Several mechanisms are thought to result in self-reinforcement as tensile load on the tendon increases: First, when tension is applied to a double-row repair, the shape of the bridging suture construct changes from rectangular to trapezoidal. The resulting elastic deformation of the repaired tendon produces a compressive force perpendicular to the bone surface.⁵ Second, increasing the tension on the tendon in a double-row repair causes narrowing of the angle between the superior suture material and the bone (Fig. 1). The suture material then wedges the tendon more tightly against the bone, increasing the footprint compression. Finally, increased suture width may increase self-reinforcement as a wider-diameter material has a greater surface area in contact with the tendon, augmenting the other 2 mechanisms.¹

The biomechanical evidence of self-reinforcement in a rotator cuff model is best demonstrated by an increase in footprint contact pressure as tensile load increases.⁸ In addition, because of the increased resistance to structural failure that occurs in self-reinforcement, the yield load of the construct should approach the ultimate load.¹ For between-group comparisons, the repair construct with the greatest self-reinforcement would demonstrate a higher rate of increase in footprint contact pressure with increasing tensile load (as demonstrated by a steeper progression [slope] of footprint contact pressure) and a closer approximation of the yield load to the ultimate load.⁹ The magnitude of footprint compression may be secondarily important in the prevention of gap formation and load to failure but is not critical to the concept of self-reinforcement. Wider-diameter tape sutures have been shown to result in great footprint compression in a single-row repair construct.²

A comparison of self-reinforcement and footprint compression between standard- and wide-diameter suture material in double-row SutureBridge repair techniques has not been performed. The aim of this study was to compare the self-reinforcement and footprint contact pressure generated under progressive tensile loads between 2 double-row SutureBridge rotator cuff repair techniques: 1 performed with FiberWire and 1 performed with FiberTape in a knotless technique. We hypothesized that the FiberTape repair construct would have superior self-reinforcement and footprint contact pressure to the FiberWire repair construct.

Materials and methods

Footprint contact pressure, yield load, pull-to-failure load, and peak energy to failure were evaluated and compared in an ovine rotator cuff repair model using No. 2 FiberWire suture

(approximately 0.5 mm in diameter; Arthrex) and FiberTape (2 mm wide by 0.5 mm thick; Arthrex). Ten paired sheep shoulders of comparable size and weight were used. The infraspinatus tendon was used because of its biomechanical and anatomic similarities to the human supraspinatus tendon, and its use has been validated in several previous studies.^{8,9}

Each shoulder was prepared by dissection of the skin, subcutaneous tissue, and superficial layers of fascia, leaving the proximal humerus, scapula, and attached infraspinatus muscle and tendon. The infraspinatus tendon was released from its humeral insertion by sharp dissection, leaving no tendon remaining on the humerus.

After removal of the tendon, the center of the infraspinatus footprint was pinpointed with a digital caliper (Mitutoyo, Kanagawa, Japan), and a drill press was used to create an 8.5-mm bone tunnel through the center of the infraspinatus footprint. The footprint was then milled until the surface was flat to prevent inconsistent readings from an uneven surface. A 4.5-mm-diameter metal probe connected to an Instron load cell (Instron, Norwood, MA, USA) was passed through the bone tunnel and positioned 2 mm above the milled footprint. This was mounted on a 4.5- to 8-mm hole adaptor to ensure that the sensor probe was positioned centrally and occupied the entire bone tunnel. The infraspinatus tendons were repaired onto the humerus over this probe, using the techniques described in the next section. The left-sided specimen of each pair was repaired with FiberTape, whereas the right shoulder was repaired with FiberWire.

Repair technique

Two medial-row 4.75-mm SwiveLock anchors (Arthrex) loaded with either FiberWire suture or FiberTape were inserted just lateral to the articular margin. Two lateral pilot holes were punched 1 cm lateral to the lateral aspect of the infraspinatus insertion. The sutures were passed in a horizontal-mattress fashion 12 mm from the lateral tendon edge with a Scorpion suture passer (Arthrex). The suture pair from each anchor was tied with a double-throw surgeon's knot, followed by 5 alternating half-hitches, in a horizontal-mattress fashion (Fig. 2). The FiberTape was left untied.

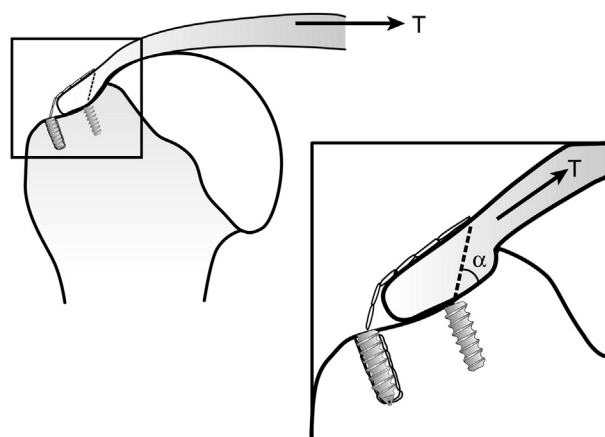


Figure 1 Wedge effect. As the load (T) increases, the angle (α) decreases, wedging the tendon more tightly between the suture and bone. (Reprinted with permission from Burkhart et al.¹)

One suture from each anchor was passed through the eyelet of a 4.75-mm SwiveLock anchor that was then inserted into the anterior lateral-row hole while tension was held on the suture ends. The remaining sutures were passed into another SwiveLock anchor inserted into the posterior lateral-row hole. This same procedure was repeated for the infraspinatus repair with FiberTape.

Biomechanical testing

Footprint compression

The protocol used for biomechanical analysis was derived from previous investigations conducted at our institute.⁸ A multidirectional vice grip with tilting function and its supporting column were used to position and secure the humerus.

Tension was applied to the repaired infraspinatus tendon by passing a hook through a hole that was punched at the medial border of the scapula, at the level of the infraspinatus muscle belly. Sets of calibrated weights were attached to the hook via a steel cable and pulley system. A counterbalance hook was used to secure the specimen against the calibrated weights and prevent shifting of the humerus (Fig. 3).

Footprint contact pressure was measured after applying increasing amounts of tension on the repaired tendon (10-60 N). The contact pressure recorded was calculated as the difference between the compression under load and the compression force with no load applied to the tendon. A wooden column with a series of pulleys attached at different heights was constructed to facilitate pressure testing at different abduction angles. These pulleys were located to create a force vector at 0°, 20°, and 40° of abduction.

Each abduction angle was tested individually. Contact pressures were measured via a computer connected to the load cell (10-kN Dynacell; Instron).

Pull to failure

After the contact pressure was tested, each specimen was labeled and stored at -20° before pull-to-failure testing. Pull-to-failure tests were performed with a mechanical tensile testing machine (Instron 8874) with a 10-kN Dynacell. The humeral specimens were secured to a baseplate with an 8-mm bolt. The infraspinatus tendons were secured with tendon-grasping clamps that pulled in a direction perpendicular to the sagittal plane and parallel with the transverse plane of the tendon. The repairs were tested with the direction of pull at 90° to the humeral shaft. The specimens were preloaded at 10 N for 30 seconds (the baseline tension for normal infraspinatus tendons); the repaired tendon was then pulled at 1.25 mm/s to failure, with the data captured at 100 Hz on the computer. The mode of failure was recorded for each specimen. Repair stiffness was calculated from the gradient of the linear section of the load-displacement curve with MATLAB software (R2009; The MathWorks, Natick, MA, USA). Tendon displacement was obtained from clamp-to-clamp displacement. No tendon slippage was observed during pull-to-failure testing; this was confirmed by checking the grip pattern of the tendon at the serrated clamp surface after testing. The total energy to failure was calculated from the area under the load-displacement curve by use of the trapezoidal rule with MATLAB software.

Statistical analysis

Differences in footprint contact pressures and load to failure between the FiberWire and FiberTape repair constructs were analyzed using 1-way analysis of variance with corrections for multiple comparisons via the Student-Newman-Keuls method. A paired *t* test was also used for comparisons between abduction angles and between loads for a given repair material. The progression (slope) of footprint contact pressure vs. load was compared between the 2 repair groups. For each abduction angle, the slopes for force and pressure for each specimen were averaged; the ratio of the averages (FiberTape slope average to FiberWire slope average) was calculated.

Results

Footprint dimensions and tendon thickness

The mean anterior-posterior footprint length of the specimens used in the FiberWire repair group was 22 ± 1.3 mm, and the mean medial-lateral footprint dimension was 15 ± 1.9 mm. The mean anterior-posterior footprint dimension of the specimens used in the FiberTape repair group was 22 ± 3.3 mm, and the mean medial-lateral footprint dimension was 16 ± 1.6 mm. The mean tendon thickness was 3.1 ± 0.2 mm in the FiberWire repair group and 3.1 ± 0.1 mm in the FiberTape repair group.

Self-reinforcement

In the neutral position, a progressive increase in tensile load on the repair (from 10 to 60 N) resulted in a progressive increase in footprint contact pressure for both the FiberWire and FiberTape groups. The progression (slope) of footprint contact pressure was greater in the FiberTape repair group (rate of slope [progression], 1.13 in FiberTape repair group vs. 0.67 in FiberWire repair group; ratio of FiberTape to FiberWire, 1.68; $P = .00035$) (Fig. 4).

At 20° of abduction, a progressive increase in footprint contact pressure with increasing load was observed only in the FiberTape group. At 40° of abduction, no increase in footprint contact pressure with increasing load was seen in either repair group (Table I).

Footprint contact pressure

In both repair constructs, the highest values for footprint contact pressure were seen at 0° of abduction. In this neutral position, no difference in the footprint compression was found between the repair constructs. At 20° of abduction, a higher footprint contact pressure was noted in the FiberTape group at all applied loads. At 40° of abduction, a significant difference between the FiberTape and FiberWire groups was only found when 10 N of tension was applied (Table I).

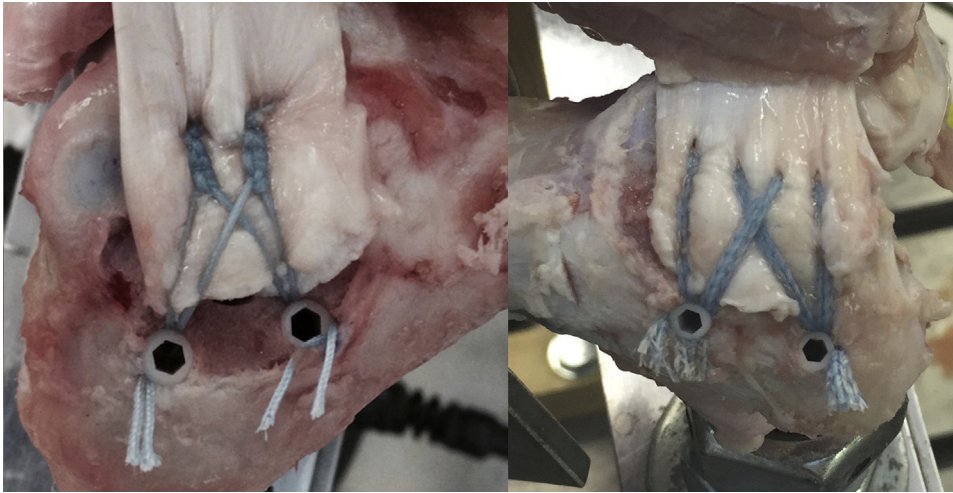


Figure 2 Photographs showing FiberWire (*left*) and FiberTape (*right*) repair constructs.

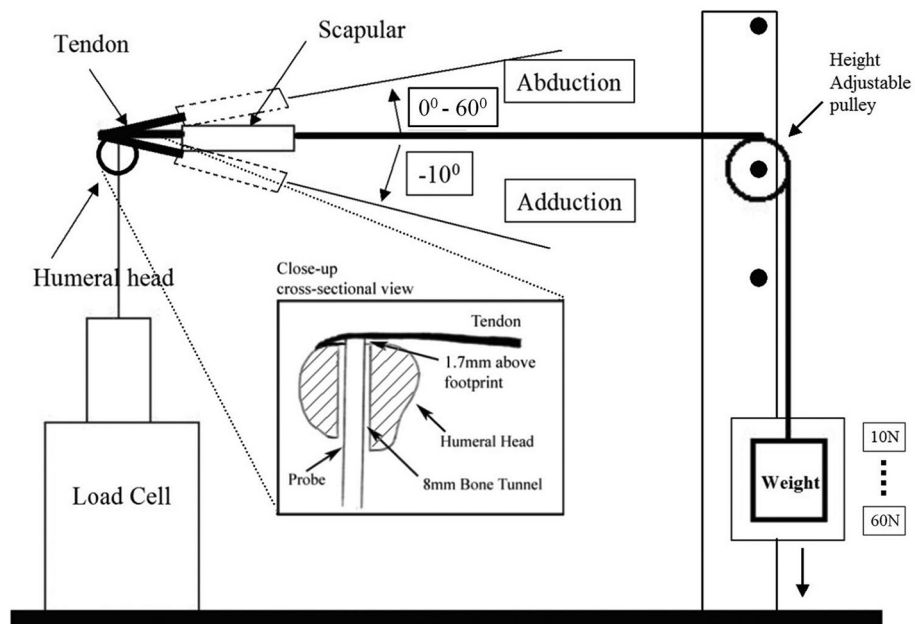


Figure 3 Apparatus for testing pull to failure, peak load, yield load, and total energy.

In the FiberWire group, as the arm was abducted from 0° to 20°, a decrease in contact pressure was observed with 20, 30, 40, 50, and 60 N of tension applied. No difference in footprint contact pressure was observed when abduction was increased from 20° to 40° in the FiberWire group. No decrease in footprint pressure was noted as the arm was abducted from 0° to 40° in the FiberTape group for all tensions applied.

Pull to failure

No significant difference in pull to failure, peak load, or total energy was found between the FiberTape and

FiberWire groups. The FiberTape group had an increased yield load compared with the FiberWire group (252 N vs. 165 N, $P = .02$), but no difference between the yield load and the ultimate load to failure was noted in the FiberTape group compared with the FiberWire group (63.4 ± 53.5 N vs. 97.6 ± 48.9 N, $P = .15$) (Table II).

Mode of failure

The failure mode of the FiberWire repair group was predominantly suture cutting through the repair tendon under load (90%, 9 of 10 specimens), whereas 1 repair failed via anchor pullout at the medial row (10%, 1 of 10). The failure

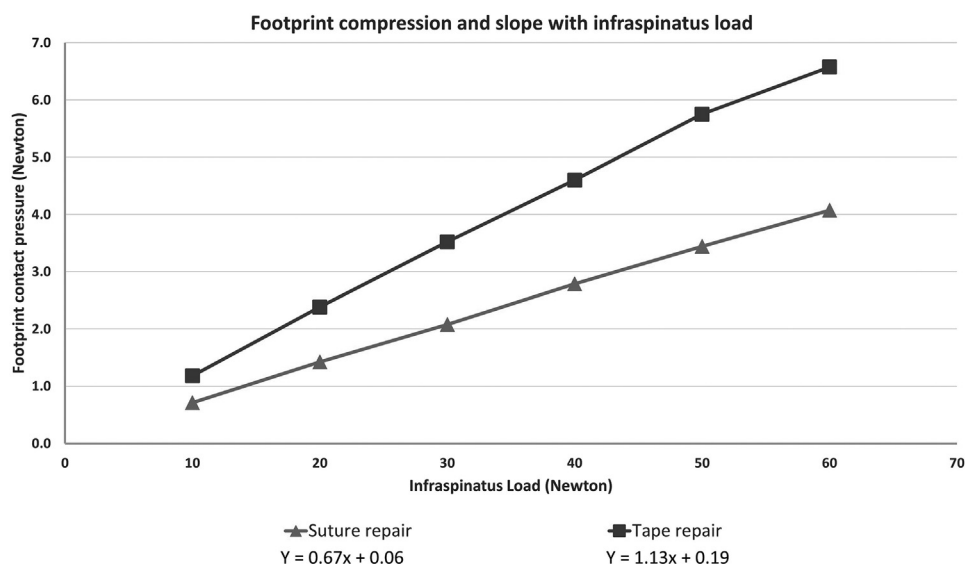


Figure 4 Difference in footprint compression between FiberWire and FiberTape repair constructs as infraspinatus load is increased.

mode of the FiberTape repair group was similar to that of the FiberWire repair group, with suture cutting through the repair tendon in 90% of specimens (9 of 10) and 1 repair failing via anchor pullout at the lateral row (10%, 1 of 10).

Discussion

This biomechanical study affirmed the self-reinforcement mechanism of double-row rotator cuff repairs in both repair constructs as progressive increases in contact pressure were seen for both FiberWire and FiberTape repairs when applied tension increased from 10 to 60 N. The degree of self-reinforcement was greater with the wider-diameter knotless FiberTape construct as evidenced by the higher rate of increase in footprint compression. Despite a higher yield load in the FiberTape group, the difference between the yield load and ultimate load was similar with the 2 techniques.

Shoulder abduction has previously been shown to diminish self-reinforcement in knotless and knotted double-row SutureBridge constructs with standard-diameter suture material.^{6,9} The results of this study confirm that shoulder abduction diminishes self-reinforcement in both constructs, although this effect was less marked in the FiberTape group. Self-reinforcement has been shown to be enhanced by using a knotless construct for the medial-row sutures in a double-row repair.⁸

No difference in footprint contact pressures was found between the 2 groups in neutral abduction. Footprint contact pressure is affected by shoulder abduction in double-row repairs.⁹ This effect has been demonstrated both in knotted and knotless constructs using standard-diameter

suture material.⁸ The decrease in footprint contact pressure with abduction in the knotted standard-diameter suture construct in this study was concordant with previous results.⁹ However, this effect was not seen in the knotless wider-diameter suture material group beyond 20° of abduction.

These results have potential implications for shoulder rehabilitation after double-row rotator cuff repair, suggesting that to maximize footprint compression, the use of early isometric strengthening and the avoidance of an abduction pillow are beneficial regardless of the double-row repair method used. Passive range into abduction should be avoided if a knotted double-row construct with standard-diameter suture material is used. The use of a knotless double-row construct with wider-diameter suture material minimizes the negative effects of shoulder abduction if it is limited to 20°. Although some differences were found in footprint compression and self-reinforcement, both constructs had similar pull-to-failure loads and peak loads.

The limitations of this study are inherent to biomechanical testing in an ovine rotator cuff model. Numerous factors such as tendon quality, bone quality, vascularity, and healing could not be assessed. In addition, there are no clinical studies to support the biomechanical concept that footprint compression is desirable after rotator cuff repair.

Conclusion

Self-reinforcement was seen in both double-row SutureBridge repairs with standard- and wide-diameter suture material but was greater in the repair with the

Table I Footprint compression in FiberWire and FiberTape groups at different abduction angles and under varying tensile loads

Applied load, N	0°			20°			40°		
	FiberWire	FiberTape	P value	FiberWire	FiberTape	P value	FiberWire	FiberTape	P value
10	1.22 ± 0.64	1.41 ± 0.91	.61	0.55 ± 0.19	1.22 ± 1.08	.08	0.37 ± 0.32	0.92 ± 0.72	.05
20	2.20 ± 0.83	3.06 ± 1.80	.19	1.10 ± 0.26	2.38 ± 1.79	.05	0.98 ± 0.43	1.71 ± 1.31	.12
30	3.12 ± 1.13	4.58 ± 2.72	.14	1.65 ± 0.58	3.48 ± 2.30	.03	1.46 ± 0.43	2.50 ± 1.94	.13
40	4.10 ± 1.29	5.92 ± 3.38	.14	2.32 ± 0.56	4.52 ± 2.75	.03	1.95 ± 0.48	3.36 ± 2.22	.08
50	4.89 ± 1.55	7.26 ± 4.04	.11	2.93 ± 0.56	5.62 ± 3.32	.03	2.50 ± 0.45	4.37 ± 2.92	.07
60	5.87 ± 1.42	8.31 ± 4.51	.13	3.54 ± 0.63	6.35 ± 3.58	.04	2.81 ± 0.59	5.07 ± 3.26	.06

Table II Pull-to-failure tests

	FiberWire	FiberTape	P value
Pull to failure, N	262.13 ± 66.52	315.24 ± 105.47	.20
Yield load, N	164.54 ± 31.77	251.84 ± 94.11	.02
Difference: Pull to failure – Yield load, N	97.59 ± 48.93	63.41 ± 53.53	.15
Peak energy, Nm	2.12 ± 0.76	2.53 ± 1.22	.38
Total energy, Nm	3.95 ± 1.04	4.49 ± 1.40	.34

wide-diameter suture material construct. Footprint compression is greater in a knotless double-row SutureBridge repair with wide-diameter suture material than in a knotted double-row SutureBridge repair with standard-diameter suture material at 20° of abduction.

Disclaimer

A grant was received from the St George Hospital Orthopaedic Department for this study.

The authors, their immediate families, and any research foundations with which they are affiliated have not received any financial payments or other benefits from any commercial entity related to the subject of this article.

References

- Burkhart SS, Adams CR, Burkhart SS, Schoolfield JD. A biomechanical comparison of 2 techniques of footprint reconstruction for rotator cuff repair: the SwiveLock-FiberChain construct versus standard double-row repair. *Arthroscopy* 2009;25:274-81. <https://doi.org/10.1016/j.arthro.2008.09.024>
- Liu RW, Lam PH, Shepherd HM, Murrell GAC. Tape versus suture in arthroscopic rotator cuff repair: biomechanical analysis and assessment of failure rates at 6 months. *Orthop J Sports Med* 2017;5:2325967117701212. <https://doi.org/10.1177/2325967117701212>
- Maher A, Leigh W, Brick M, Young S, Caughey M. Causes of pain and loss of function in rotator cuff disease: analysis of 1383 cases. *ANZ J Surg* 2017;87:488-92. <https://doi.org/10.1111/ans.13870>
- Murrell GAC. Advances in rotator cuff repair—undersurface repair. *Tech Shoulder Elbow Surg* 2012;13:28-31. <https://doi.org/10.1097/BTE.0b013e31823ba3dd>
- Park MC, McGarry MH, Gunzenhauser RC, Benefiel MK, Park CJ, Lee TQ. Does transosseous-equivalent rotator cuff repair biomechanically provide a “self-reinforcement” effect compared with single-row repair? *J Shoulder Elbow Surg* 2014;23:1813-21. <https://doi.org/10.1016/j.jse.2014.03.008>
- Park MC, Pirolo JM, Park CJ, Tibone JE, McGarry MH, Lee TQ. The effect of abduction and rotation on footprint contact for single-row, double-row, and modified double-row rotator cuff repair techniques. *Am J Sports Med* 2009;37:1599-608. <https://doi.org/10.1177/0363546509332506>
- Perry SM, Getz CL, Soslowsky LJ. Alterations in function after rotator cuff tears in an animal model. *J Shoulder Elbow Surg* 2009;18:296-304. <https://doi.org/10.1016/j.jse.2008.10.008>
- Smith GCS, Bouwmeester TM, Lam PH. Knotless double-row SutureBridge rotator cuff repairs have improved self-reinforcement compared with double-row SutureBridge repairs with tied medial knots: a biomechanical study using an ovine model. *J Shoulder Elbow Surg* 2017;26:2206-12. <https://doi.org/10.1016/j.jse.2017.06.045>
- Smith GCS, Lam PH. Shoulder abduction diminishes self-reinforcement in transosseous-equivalent rotator cuff repair in both knotted and knotless techniques. *Knee Surg Sports Traumatol Arthrosc* 2018;26:3818-25. <https://doi.org/10.1007/s00167-018-4999-y>